The Magellanic System: Stars, Gas, and Galaxies
Proceedings IAU Symposium No. 256, 2008
Jacco Th. van Loon & Joana M. Oliveira, eds.

DOI: 00.0000/X000000000000000X

Dark Clouds in the Small Magellanic Cloud

Min-Young Lee[1], Snežana Stanimirović[1], Jürgen Ott[2], Alberto D. Bolatto[3], J.Th. van Loon[4], K.E. Devine[1], J.M. Oliveira[4], P.A. Jones[5] and M.R. Cunningham[5]

[1]Department of Astronomy, University of Wisconsin-Madison, 475 North Charter Street, Madison, WI 53706, USA
email: lee@astro.wisc.edu and sstanimi@astro.wisc.edu
[2]National Radio Astronomy Observatory, USA
[3]Department of Astronomy, University of California-Berkeley, USA
[4]Astrophysics Group, Lennard-Jones Laboratories, Keele University, UK
[5]School of Physics, University of New South Wales, Australia

Abstract. We search for high-extinction regions in the Spitzer 24 μm image of the Small Magellanic Cloud (SMC) by generating an image of the decremental contrast against the modeled diffuse infrared background. Several interesting high-decremental contrast regions are identified and most of them are near active star-forming regions. For one of the identified clouds we obtained millimeter observations of several molecular species but did not detect any emission. While tracing a moderately high extinction, our clouds have significantly lower abundance of NH_3 than what is found in Galactic molecular clouds. The high-decremental contrast regions in the SMC most likely trace moderately warm and dense molecular medium, not well traced by CO, but with a significant abundance of H_2.

Keywords. Magellanic Clouds, galaxies: ISM, infrared: ISM

1. Introduction

The SMC is one of the closest neighbors of the Galaxy. It is a low mass, gas rich, dwarf irregular galaxy, located at a distance of approximately 60 kpc from the Galactic center. With a metallicity 5 times lower than Galactic (Dufour 1975), and an interstellar radiation field 4−10 time higher than in the Solar neighborhood (Lequeux et al. 1994), the SMC offers a unique insight into the physics of the primitive interstellar medium (ISM) common in high-redshift galaxies.

The main goal of this study is to investigate how the specific ISM environment in the SMC influences properties of the high-extinction regions. In the Galaxy, the highest extinction regions stand out easily against the bright Galactic background at mid-infrared wavelengths. Numerous Infrared Dark Clouds (IRDCs) were identified this way (Egan et al. 1998). Further millimeter and submillimeter observations confirmed that the IRDCs are dense ($n > 10^5$ cm^{-3}) and cold ($T < 20$ K), and are most likely the precursors of high-mass protostars and protoclusters (Carey et al. 1998).

To select potential high-extinction regions in the SMC we analyze the SMC 24 μm image, obtained with the Spitzer Space Telescope (SST; Bolatto et al. 2007), using the unsharp-masking technique. The unsharp-masking technique has been widely used for studies of high-extinction regions in the Galaxy (e.g. Simon et al. 2006), but has never been applied on IR images of the Magellanic Clouds. To constrain physical properties of selected regions we performed millimeter observations. In this paper we briefly summarize the main results from this project.

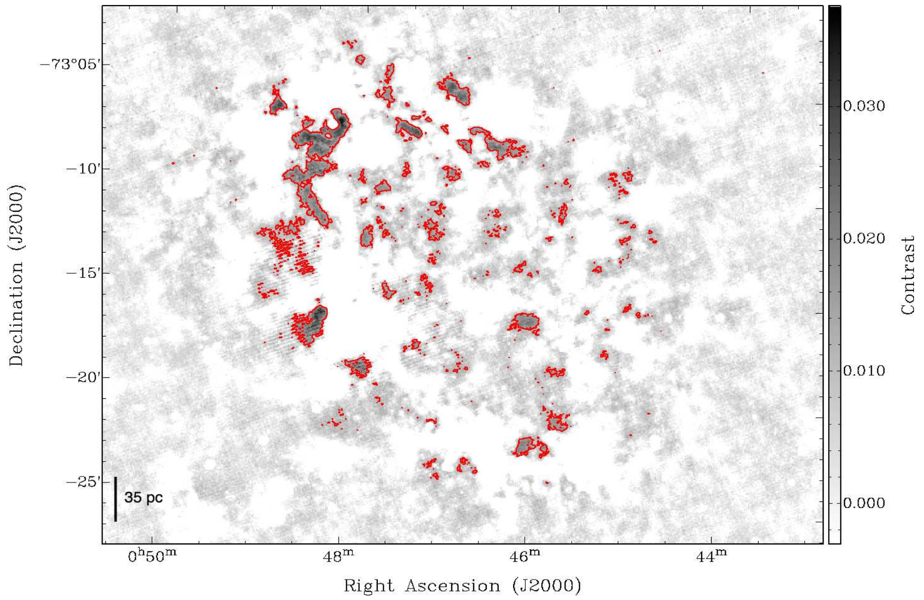

Figure 1. The 24 μm contrast image of the SMC bar region, defined as contrast = (background - original image)/background. High-decremental contrast regions have positive values and are shown in black. The overlaid contours represent pixels with the signal-to-noise ratio equal to 5.

2. Search for High-Extinction Regions

We applied a method similar to that of Simon et al. (2006), who cataloged 10,931 Galactic IRDCs based on the Midcourse Space Experiment (MSX) images at 8 μm. To model the diffuse 24 μm background we applied the median filter (kernel size = 63 pixels; full details are provided in Lee et al. in preparation). We then generated the contrast image c, defined by c = (background − original image)/background. By this definition, regions having lower surface brightness against the diffuse background have positive values in the contrast image. Considering that our linear resolution is 12 pc, we are sensitive to clouds with a size similar to, or larger than, the largest Galactic IRDCs. Finally, we identified the high-decremental contrast regions as contiguous regions with a signal-to-noise ratio $c/\Delta c \geqslant 5$. The contrast error, Δc for a particular pixel was calculated by dividing 1σ noise in the Spitzer 24 μm image (0.06 MJy sr^{-1}) by the pixel value in the modeled background.

The 24 μm contrast image of the SMC bar region is shown in Figure 1, with $c/\Delta c = 5$ contours delineating boundaries of the high-contrast regions. In general, the fractional decrement across the SMC is very small ($\sim$ 4%). This is much smaller that what is typically found in the Galaxy, with the highest contrast regions corresponding to IRDCs having fractional decrements $> 30 - 60$%. About a dozen discrete contiguous regions with $> 5\sigma$ are easily noticeable, ranging in size from 15 to 50 pc. A zoom-in of the south bar region is shown in Figure 2, with several prominent molecular clouds (LIRS36, LIRS49, and SMCB2) shown with contours of CO(J=1–0) emission (Mizuno et al. 2001). Interestingly, most of the high-contrast regions are distributed in peripheral areas of CO(J=1–0) clouds. To explain measured contrast values we modeled the IR intensity at 24 μm as having equal contributions from emission behind and in front of the clouds. This allowed us to estimate the cloud optical depth. The corresponding extinction of contrast clouds is moderately high, $A_V \sim 1$ mag (Lee et al. in preparation), considering that the molecular peaks in the SMC have $A_V = 1 - 2$ mag (Leroy et al. 2007).

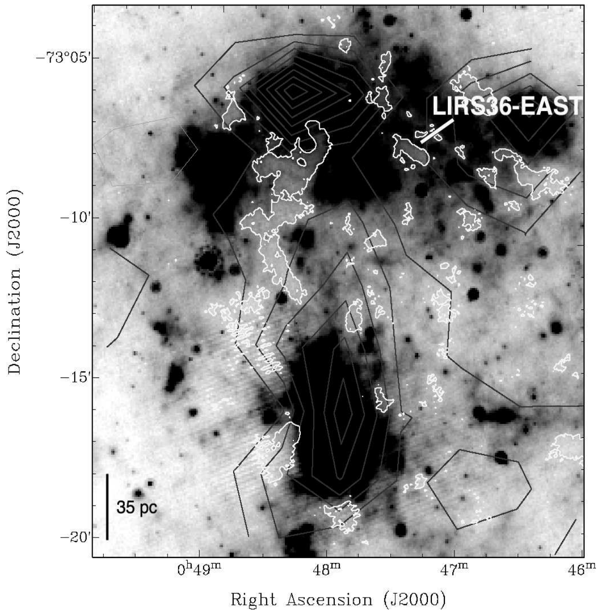

Figure 2. The 24 μm image of the SMC bar region overlaid with the CO(J=1–0) contours (Mizuno et al. 2001) in blue. The high-contrast regions are shown with yellow contours. LIRS36 is the molecular cloud centered at RA 00:46:30, Dec –73:07.

3. Search for Molecules

To investigate physical properties of our high-contrast clouds, we searched for several molecular species in the direction of one of the candidates, called LIRS36-east throughout this work (Figure 2). LIRS36-east stands out in the Spitzer 24 μm image as a silhouette against the more diffuse surrounding emission. Observations of NH_3(1,1) and (2,2) transitions were performed with the Australia Telescope Compact Array (ATCA). We also used the 22-m Mopra single dish telescope to search for N_2H^+(J=1–0), HNC(J=1–0), HCO^+(J=1–0), and HCN(J=1–0) spectral lines.

We did not detect emission from any of the six lines. The upper limits to column densities of NH_3(1,1) and HCO^+ are listed in Table 1. In the case of NH_3, our 3σ upper limit is similar to the only detection of ammonia in the Large Magellanic Cloud (Ott et al. in preparation). For HCO^+ our 3σ upper limit is two times lower than the detection by Chin et al. (1998) in the direction of LIRS36. The non-detections of NH_3 and HCO^+ suggest a very low abundance of cold and dense gas in the direction of LIRS36-east.

4. Discussion and Conclusions

High-decremental contrast regions in the SMC, revealed through the unsharp-masking of the Spitzer 24 μm image, are mainly larger and have a much lower fractional intensity decrement than what is found in the Galaxy. While the size of the high-contrast clouds is limited by the angular resolution of the 24 μm image, the lower intensity contrast is partially due to a significantly lower IR diffuse emission in the SMC, as well as a large line-of-sight depth.

Can some of our high-contrast regions represent IRDCs? It has been shown that CO clouds in the LMC and SMC are most likely much smaller than in the Galaxy (Lequeux et al. 1994). Therefore, the column densities in Table 1 may be significantly underestimated.

Table 1. Upper Limits to Column Densities of Molecular Species in LIRS36-east

Molecule	Transition	Frequency (MHz)	3σ Level[1]	Column Density (cm^{-2})
NH_3	(1,1)	23694.506	3.2	$< 4.7 \times 10^{12}$
HCO^+	J=1–0	89188.518	48	$< 3.5 \times 10^{11}$

[1] The units of 3σ levels are mJy Beam^{-1} for NH_3 and mK for HCO^+.

If we correct for the beam dilution caused by the presence of small clumps (~ 1 pc) within our telescope beam, the upper limit to the NH_3 column density of LIRS36-east reaches 3.5×10^{14} cm^{-2}. While this is a high-extinction cloud at 24 μm (for the SMC standards), it has a significantly lower NH_3 column density than what is found for Galactic IRDCs ($> 10^{15}$ cm^{-2}).

One particularly interesting aspect of the high-contrast regions is that they are located in the periphery of CO clouds, with either very weak or no CO(J=1–0) emission. In addition, based on the H_2 surface density map of Leroy et al. (2007), the high-contrast regions ($A_V \sim 1$ mag) have a significant amount of H_2. This is in agreement with Rubio et al. (2000) who found that in the star-forming region N66 CO exists only in regions with $A_V > 1$ mag, while H_2 requires $A_V > 0.1$ mag. This is mainly due to the selective photodissociation of CO in lower density regions. In the SMC bar region, Bolatto et al. (2005) found the coexistence of cold and dense ($T = 10 - 60$ K, $n = 10^{4-5}$ cm^{-3}) gas with a warmer and moderately dense component ($T = 100 - 300$ K, $n = 10^{2-3}$ cm^{-3}). All of this suggests that the 24 μm high-contrast regions most likely trace moderately warm and dense molecular gas, with highly photodissociated CO, but with a significant abundance of H_2.

Acknowledgements

This work is based on observations made with the *Spitzer Space Telescope*, operated by the Jet Propulsion Laboratory, California Institute of Technology, under a contract with NASA. This research is supported by NASA-JPL Spitzer grant 1289519. The Australia Telescope Compact Array and Mopra telescope are funded by the Commonwealth of Australia as a National Facility managed by CSIRO as part of the Australia Telescope. M.-Y. Lee acknowledges support from IAU grant and AAS international travel grant.

References

Bolatto, A.D., Israel, F.P., & Martin, C.L. 2005, *ApJ*, 633, 210

Bolatto, A.D., Simon, J.D., Stanimirović, S., et al. 2007, *ApJ*, 655, 212

Carey, S.J., Clark, F.O., Egan, M.P., Price, S.D., Shipman, R.F., & Kuchar, T.A. 1998, *ApJ*, 508, 721

Chin, Y.N., Henkel, C., Millar, T.J., Whiteoak, J.B., & Marx-Zimmer, M. 1998, *A&A*, 330, 901

Dufour, R.J. 1975, *ApJ*, 195, 315

Egan, M.P., Shipman, R.F., Price, S.D., Carey, S.J., Clark, F.O., & Cohen, M.A. 1998, *ApJ*, 494, L199

Lequeux, J., Le Bourlot, J., Des Forets, G.P., Roueff, E., Boulanger, F., & Rubio, M. 1994, *A&A*, 292, 371

Leroy, A., Bolatto, A., Stanimirovíc, S., Mizuno, N., Israel, F., & Bot, C. 2007, *ApJ*, 658, 1027

Mizuno, N., Rubio, M., Mizuno, A., Yamaguchi, R., Onishi, T., & Fukui, Y. 2001, *PASJ*, 53, L45

Rubio, M., Contursi, A., Lequeux, J., Probst, R., Barba, R., Boulanger, F., Cesarsky, D., & Maoli, R. 2000, *A&A*, 359, 1139

Simon, R., Jackson, J. M., Rathborne, J.M., & Chambers, E.T. 2006, *ApJ*, 639, 227